MULTIMODAL ULTRASOUND INCLUDING VIRTUAL TOUCH IMAGING QUANTIFICATION FOR DIFFERENTIATING CERVICAL LYMPH NODES

HOLGER RÜGER,[*,1] GEORGIOS PSYCHOGIOS,[*,†,1] MONIKA JERING,[*] and JOHANNES ZENK[*]

* Department of Otorhinolaryngology, Head and Neck Surgery, University of Augsburg, Augsburg, Germany; and † Department of Otorhinolaryngology, Head and Neck Surgery, University of Ioannina, Ioannina, Greece

INTRODUCTION

High-resolution ultrasound (US) and color Doppler US are crucial in the differentiation of unclear mass lesions of the neck, especially in patients with head and neck cancer (Bozzato 2015a, 2015b). Previous studies have described criteria for the evaluation of the entity of cervical lymph nodes (LNs) as follows: tumor margins, shape, lymph node (LN) diameter including the Solbiati index, presence of a hilar sign, perfusion pattern and homogeneity (Rubaltelli et al. 1990; Steinkamp et al. 1995; Bozzato 2015a, 2015b; Turgut et al. 2017).

Sonographic features of benign LNs include an oval shape, well-defined margins, homogeneity and hilar perfusion. Furthermore, a benign LN is characterized by a diameter <10 mm in the short axis and a fatty hilum. On the other hand, up to 50% of metastatic lymph nodes (MLNs) also have a hyper-echoic hilar structure. LNs with ill-defined tumor margins raise the suspicion of extranodal metastatic spread (Lenghel et al. 2012; McQueen and Bhatia 2018). A considerable advantage of head and neck sonography, particularly in the case of tumor diseases, is the possibility of close monitoring and documentation of the changing dynamics of LN size and sonomorphology of suspicious LNs without any side effects, as well as the pre-operative examination (Zhao et al. 2017; Psychogios et al. 2019). The use of contrast-enhanced US to differentiate benign from malignant LNs may be helpful in addition to 2-D US and color Doppler but has currently not been validated as an established tool in the clinical setting (Zenk et al. 2005; Azizi et al. 2015, 2016; Desmots et al. 2016). Despite all these criteria, sonographic entity differentiation remains a challenge and is not sufficiently specific (Benzel et al. 1996; Lenghel et al. 2012; McQueen and Bhatia 2018).

The development of elastography and Virtual Touch imaging quantification (VTIQ) has made it possible to measure the elasticity and stiffness of tissue qualitatively and quantitatively using shear waves. VTIQ is a 2-D shear wave technology generated by acoustic radiation force impulses (ARFIs) (Rosen et al. 2008; Tozaki et al. 2013; Azizi et al. 2016; Zhang et al. 2016). Elastography and VTIQ use shear waves to measure the mechanical properties of tissue in terms of stiffness and translate them into a color-coded image (Fig. 1). In the

Address correspondence to: Holger Rüger, Department of Otorhinolaryngology, Head and Neck Surgery, University of Augsburg, Augsburg, Germany. E-mail: rueger.holger@gmx.de

[1] Holger Rüger and Georgios Psychogios contributed equally to this article.

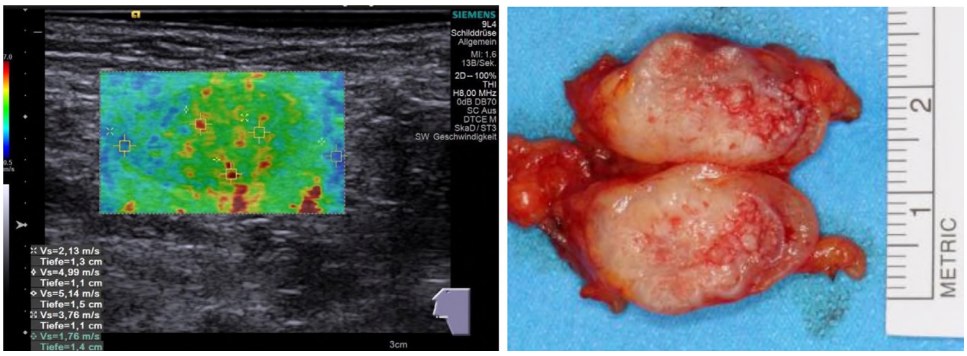

Fig. 1. Left: Oval-shaped cervical lymph node with multiple quantitative measurements of shear wave velocity made using Virtual Touch tissue imaging quantitation with a maximum shear wave velocity of 5.14 m/s inside the node. Right: Photograph of the lymph node after surgical excision.

case of soft tissue, it is easy to deflect or shift the shear waves so that lower velocities can be measured. These shear wave velocities (SWVs) can be displayed independently of the surface pressure at the transducer by the examiner (Fig. 1). As shear waves do not propagate in fluid, no signal can be measured in cystic lesions (Matsuzuka et al. 2015; Azizi et al. 2016; Desmots et al. 2016; Zhao et al. 2017).

Elastography and VTIQ have been validated in previous studies on breast diseases, parotid glands and thyroid carcinomas and have revealed an association between malignancy and higher SWVs (Klotz et al. 2014; Azizi et al. 2015; He et al. 2017; Mansour et al. 2017, 2019; Pu et al. 2017; Heine et al. 2018; Guruf et al. 2019). Depending on the cutoff of the maximum SWV within an LN, the positive and negative predictive values can reach 52.44% and 94.15%, respectively (Azizi et al. 2016). In a meta-analysis of eight studies, malignant LNs were stiffer than benign nodes, and the SWV for diagnosing malignant cervical LNs had a sensitivity of 81% and a specificity of 85% (Suh et al. 2017). The diagnostic accuracy of SWV using Toshiba shear wave elastography for differentiating metastasis from lymphoma was between 80.7% and 83.9% (Chae et al. 2019). He et al. (2017) suggested that VTIQ using ARFIs and Toshiba shear wave elastography are comparable and reproducible for diagnosing thyroid nodules.

The feasibility of using elastography in the head and neck area has not yet been determined (Mantsopoulos et al. 2015; Desmots et al. 2016). One reason is the complicated anatomy, which leads to artifacts near the lower jaw, thyroid cartilage and large neck vessels (Klintworth et al. 2012). Moreover, the few prospective studies in this area have methodological problems, as they usually do not compare the histopathological results of the neoplasms but the results of fine-needle aspiration biopsy, which are known to have disadvantages such as sampling errors and analytic uncertainty (Tan et al. 2010; Cheng et al. 2016). The aim of this study was to determine a combined target value of area and SWV that can be used to predict or exclude a malignancy. Our hypothesis is that the additional use of VTIQ can improve the entity determination of cervical LNs.

METHODS

This prospective study was conducted between June 2017 and June 2019 at the Department of Otorhinolaryngology, Augsburg University Hospital, Augsburg, Germany. The study was approved by the local ethics committee (2017/19), and informed consent was obtained from all patients.

This study included 108 patients who presented with a cervical mass with and without head and neck squamous cell carcinoma. All patients with unclear cervical lymphadenopathy who underwent pre-operative US screening by one of the clinical investigators were included in the study. Detailed US documentation of the LNs using 2-D sonography, color Doppler US and elastography with VTIQ was performed. Furthermore, video documentation of the suspected LN was conducted.

The exclusion criteria were as follows: age <18, no known histology, condition after radiotherapy of the neck region, malignant lymphoma, lack of patient's ability to consent and impossibility to locate and remove the suspected LN intra-operatively.

VTIQ is based on the principle of ARFI technology. Tissue is compressed using multiple high-intensity, acoustic push beams from a US transducer. By measurement of the local displacement of tissue *via* the acoustic pulse, the propagation of transverse shear waves can be tracked. The stiffer the tissue is, the higher is the SWV (Zhang et al. 2012). SWV in human tissue is in the range $1-10$ m/s. By creation of a color-coded shear wave image at the same time in VTIQ, it is possible to quantify SWV in a precise anatomic region of interest, with a pre-

defined size of 1.5 mm. Moreover, we used the quality map to verify sufficient magnitude and to distinguish between soft and stiff areas (Tozaki et al. 2013).

Pre-operatively, all patients were examined according to the same protocol with an Acuson S2000 US system (Siemens Medical Solution, Erlangen, Germany). The measurements were performed using a 9-MHz linear array transducer, color Doppler examination and shear wave elastography using VTIQ. Patients were asked to avoid swallowing and to hold their breath for a few seconds while the image was acquired. VTIQ shear wave elastography was performed three times in each patient by one investigator (G.P. or J.Z.). Both are well-experienced head and neck sonographers.

The features documented were 2-D sonography (horizontal, vertical) with accurate tumor size measurements, color Doppler US and complete LN mapping of the SWV *via* VTIQ. The localization of the cervical LN was marked on the skin, and the adjacent anatomic structures were exactly described.

As illustrated in Figure 1, three quantitative measurements of SWV were made at distinctive sites and repeated three times: normal tissue outside the lesion (as a reference); minimal SWV inside the lesion; maximum SWV inside the lesion. Each SWV value was defined as the median of the three measurements within and outside the lesion. Normal tissue outside the lesion was used as a reference.

On the basis of the histopathological results, patients were divided into two groups, those with benign lesions and those with head and neck squamous cell metastatic LNs. Stiff tissue was defined as an SWV $\geq$6 m/s, and soft tissue was defined as an SWV $\leq$3.5 m/s. The velocity measured at different areas was categorized into three groups ($<$30%, 30%$-$69% and $\geq$70% of the whole neoplasm) to simplify the exact classification compared with two groups only.

If there was a single suspected LN, extirpation under general anesthesia was performed. If the patient underwent complete neck dissection, the most suspicious LN was pre-operatively documented and classified at the correct cervical level. The removed LN was sent separately from the remaining neck preparation for histologic examination. The surgical procedure was performed by the same investigator who performed US pre-operatively to eliminate the danger of false LN selection. The size of the extirpated LN was compared with the size measured by US pre-operatively to verify the correct selection. Additionally, intra-operative photo documentation was performed. All surgical pathology results were compared with the pre-operative US examination results.

The following questions were examined and documented pre-operatively:

- What is the mean SWV outside the cervical LN?
- What is the average maximum SWV within the cervical LN?
- What percentage of the elastographically measured area of the LN is stiff, which is defined as an SWV $\geq$6 m/s, or soft, defined as an SWV $\leq$3.5 m/s, in VTIQ?

All quantitative data are expressed as the mean $\pm$ standard deviation for continuous variables and as percentages for categorical variables. Chi-square and Fisher's exact tests were performed for group testing of categorical variables. For continuous variables, *t*-tests were used for comparisons among groups. Moreover, we performed logistic regression analysis. All statistical analyses were performed using SPSS Version 25 (IBM, Armonk, NY, USA), with p values $<$0.05 considered to indicate statistical significance.

RESULTS

In this prospective study, 108 LNs from 108 patients were eligible for inclusion. There were a total of 57 benign LNs and 51 malignant LNs. We performed bivariate and multivariate analyses.

Among the 2-D US characteristics, well-defined margins were more prevalent among benign LNs (89.5%) than among malignant LNs (43.1%). Hilar blood flow was predictive of benign LNs, and peripheral and diffuse flow were predictive of malignant LNs (Table 1).

The maximum SWV (average $\pm$ standard deviation) within the lesions in the malignant group was 8.3 $\pm$ 1.7 m/s, with a minimal SWV of 4.1 $\pm$ 1.2 m/s. Among benign LNs, the average maximum SWV was 4.1 $\pm$ 1.8 m/s, and the average minimal SWV was 2.7 $\pm$ 0.8 m/s. Both maximum and minimum SWVs within the cervical masses significantly differed between benign masses and MLNs ($p < 0.001$) (Table 2).

Table 1. Bivariate analysis of general ultrasound characteristics

Variable	Benign	Malignant	*p* Value
No. of lesions	57	51	
Sex (male)	64.9%	70.6%	0.545
Age	51.3 $\pm$ 21.1	68.2 $\pm$ 11.9	**$<$0.001**
Axis ratio $>$0.5 (round)	24.6%	43.1%	0.065
Margins (well-defined)	89.5%	43.1%	**$<$0.001**
Perfusion pattern			**$<$0.001**
None	12.2%	7.8%	
Hilar	61.4%	5.9%	
Peripheral	19.3%	64.7%	
Diffuse	7.0%	21.6%	

Data are expressed as the mean $\pm$ standard deviation or percentage. Boldface indicates significant differences.

Table 2. Bivariate analysis of lesion characteristics based on Virtual Touch imaging quantification

Variable	Benign	Malignant	*p* Value
Shear wave velocity			
Maximum inside lesion	4.1 ± 1.8	8.3 ± 1.7	<**0.001**
Minimum inside lesion	2.7 ± 0.8	4.1 ± 1.2	<**0.001**
Outside lesion	2.2 ± 0.6	2.3 ± 0.6	0.349
Area ≥6 m/s			
0–29%	94.7% (54/57)	25.5% (13/51)	<**0.001**
30%–69%	5.3% (3/57)	47.1% (24/51)	
70%–100%	0% (0/57)	27.5% (14/51)	
Area ≤3.5 m/s			
0–29%	10.5% (6/57)	70.6% (36/51)	<**0.001**
30–69%	17.5% (10/57)	27.5% (14/51)	
70–100%	71.9% (41/57)	2.0% (1/51)	

Data are expressed as the mean ± standard deviation or percentage (numbers) respectively. Boldface indicates significant differences.

The categorized areas with SWVs ≥6 m/s and ≤3.5 m/s significantly differed for soft and stiff lesions ($p < 0.001$) (Table 2).

As described, we divided the LNs into three groups based on the intralesional area of SWV ≤3.5 m/s. Group 1 contained a total of 42 LNs, with 6 benign LNs (14.3%) and 36 malignant LNs (85.7%). In group 2, 10 of 24 LNs (41.7%) were benign, and 14 (58.3%) were malignant. Group 3 had a total of 42 LNs, with 41 benign LNs (97.6%) and 1 malignant LN (2.4%) (Table 2).

We also divided the LNs into three groups based on the intralesional area of SWV ≥6 m/s. Group 1 had a total of 67 LNs, with 54 benign LNs (80.6%) and 13 malignant LNs (19.4%). In group 2, 3 of 27 LNs (11.1%) were benign, and 24 (88.9%) were malignant. Group 3 had a total of 14 LNs, which were all malignant (100%) (Table 2).

The average SWV for regular cervical soft tissue outside the lesions measured with VTIQ was 2.2 ± 0.6 m/s. There was no significant difference between the two groups with respect to the SWV of tissue outside the lesion (Table 2).

Patients with malignant LNs were older than those with benign LNs. Through further statistical testing, we determined that the SWV of tissue outside the lesion did not differ with respect to age in general.

Furthermore, we performed multivariate analysis using the variable intralesional area of SWV ≤3.5 m/s.

Table 3 outlines the logistic regression analysis of the potential predictors of malignant LNs. Intralesional areas with SWVs ≤3.5 m/s of 0–29% (odds ratio [95% confidence interval]: 93.672 [8.054–1089.453]) and 30%–69% (46.280 [3.716–576.437]) were predictive of malignant LNs. The odds of predicting malignancy compared with the reference group (percentage area of SWV ≤3.5 m/s: 70%–100%) exponentially increased with a smaller percentage area of SWV ≤3.5 m/s. A blurred boundary (5.248 [1.100–25.033]) was also predictive of malignancy.

When we performed another multivariate analysis for an intralesional percentage area of SWV ≥6 m/s, our logistic regression analysis revealed numerical problems that resulted in instability of the analysis by singularities. In fact, there was no benign LN with an intralesional area of SWV ≥6 m/s of 70%–100%, which was used as the reference group. The perfusion pattern, which was statistically significant in bivariate analysis, did not reach statistical significance in multivariate analysis as a predictor of malignancy.

DISCUSSION

The aim of this prospective study was to investigate the diagnostic performance of multimodal US using VTIQ shear wave elastography in the differentiation of benign and malignant cervical LNs. Lymphoma was excluded in this study because it might be softer than

Table 3. Multivariate analysis

Covariate	Coefficient, *B*	Odds ratio	95% Confidence interval		*p* Value
Sex	−0.064	0.938	0.211–4.164		0.933
Age	0.043	1.044	0.999–1.090		0.055
Ill-defined margins	1.658	5.248	1.100–25.033		**0.038**
Perfusion pattern					
Diffuse (reference)	-	-	-	-	0.225
None	−1.450	0.234	0.012	4.624	0.340
Hilar	−2.206	0.110	0.009	1.336	0.083
Peripheral	−0.547	0.579	0.060	5.540	0.635
Area of SWV					
≤3.5 m/s (70%–100%, reference)	-	-	-	-	**0.001**
≤3.5 m/s (0–29%)	4.540	93.672	8.054	1089.453	<**0.001**
≤3.5 m/s (30%–69%)	3.835	46.280	3.716	576.437	**0.003**

SWV = shear wave velocity.
Boldface indicates significant differences.

MLNs (Okasha et al. 2014; Chae et al. 2019; Rüger et al. 2019). Furthermore, lymphomas can usually be diagnosed according to clinical signs on presentation and have a distinctive appearance in B-mode US similar to a "string of beads" (Bialek and Jakubowski 2017). The correct diagnosis of a cervical LN is essential in terms of treatment decisions and survival (Kau et al. 2000; Ferlito et al. 2002).

Both the maximum and minimum SWVs within the cervical masses were higher for MLNs than for benign masses. Previous studies have reported similar findings (Luo et al. 2011; Fujiwara et al. 2013; Cheng et al. 2016; Turgut et al. 2017). The percentage area of masses with an SWV ≥6 m/s was higher for malignant LNs. In fact, there were no benign LNs with an intralesional area of SWV ≥6 m/s of 70%–100%. The multivariate analysis identified intralesional areas of SWV ≤3.5 m/s of 0–29% and of 30%–69% as highly predictive of malignant LNs with odds ratios of 93.7 and 46.3, respectively. Zhang et al. (2015) reported a higher percentage area with a certain SWV for malignant LNs. The cutoff values used were an area of 45.27% and an SWV of 3.14 m/s.

Our findings indicate that an LN with an intralesional area of SWV ≤3.5 m/s of 0–29% is 93.7 times more likely to be malignant than an LN with an intralesional area of SWV ≤3.5 m/s of 70%–100%. Moreover, we could not find any benign LNs with an intralesional area of SWV ≥6 m/s of >70%. Hence, a fast diagnostic workout *via* histology or removal is mandatory in this situation.

For 270 LNs, Azizi et al. (2016) identified the best cutoff value of 2.93 m/s for predicting malignancy by performing US with the Siemens Acuson S3000 US system and using a 9 L4 Multi-D probe. Another group used 3.03 m/s as a cutoff value and obtained a sensitivity of the maximum SWV for differentiating benign and malignant LNs of 93% (Kilic and Colakoglu Er 2019). In the study by Herman et al. (2019), examination of the SWV did not add much new predictive power compared with that provided by classic US parameters.

In our study, the perfusion pattern was statistically significant in bivariate analysis. However, it did not reach statistical significance in multivariate analysis as an independent predictor of malignancy. Nevertheless, other publications have reported an association of peripheral and diffuse perfusion with malignant LNs (Bruneton et al. 1984; Ying et al. 1998; Dragoni et al. 1999).

Among the demographic characteristics, patients with malignant LNs were older than those with benign lesions. The stiffness of the regular cervical tissue outside the lesion did not exhibit any significant difference with respect to the entity of the lesion or the age itself, confirming the common fact that malignant LNs are more likely to be found in elderly patients (Cooper et al. 2009; Smith 2009; Azizi et al. 2015; Herman et al. 2019).

The strengths of this study include the prospective design and the large number of LNs examined. According to the percentage area of SWV ≤3.5 m/s of the cervical lesion, we created three groups to simplify the categorization. However, this separation made it impossible to perform receiver operating characteristic curve analysis as in other studies (Azizi et al. 2016; Cheng et al. 2016; Zhang et al. 2016). Therefore, further studies should measure the percentage area as a continuous variable.

CONCLUSIONS

Multimodal sonography with VTIQ reveals significant differences between LN metastases and benign LNs. Intralesional areas of SWV ≤3.5 m/s of 0–29% and 30%–69% are highly predictive of malignancy. Therefore, VTIQ can be a suitable tool for the entity differentiation of cervical LNs and can help us determine further treatment options.

Acknowledgments—This study was funded by DEGUM (Deutsche Gesellschaft für Ultraschall in der Medizin, Grant No. DEGUM_2018.07.03).

Conflict of interest disclosure—The authors have no conflicts of interest to declare.

REFERENCES

Azizi G, Keller JM, Mayo ML, Piper K, Puett D, Earp KM, Malchoff CD. Thyroid nodules and shear wave elastography: A new tool in thyroid cancer detection. Ultrasound Med Biol 2015;41:2855–2865.

Azizi G, Keller JM, Mayo ML, Piper K, Puett D, Earp KM, Malchoff CD. Shear wave elastography and cervical lymph nodes: Predicting malignancy. Ultrasound Med Biol 2016;42:1273–1281.

Benzel W, Zenk J, Winter M, Iro H. [Color Doppler ultrasound studies of benign and malignant lymph nodes]. HNO 1996;44:666–671.

Bialek EJ, Jakubowski W. Mistakes in ultrasound diagnosis of superficial lymph nodes. J Ultrasonogr 2017;17:59–65.

Bozzato A. [Interpretation of ultrasound findings in otorhinolaryngology: Skin, soft tissue of the neck, lymph nodes, and oncologic follow-up]. HNO 2015a;63:139–154.

Bozzato A. [Interpretation of ultrasound findings in otorhinolaryngology. Salivary glands, paraganglioma, angioma, esophagus, hypopharynx, extra cranial vessels and temporomandibular joint]. HNO 2015b;63:453–465 quiz 66–67.

Bruneton JN, Roux P, Caramella E, Demard F, Vallicioni J, Chauvel P. Ear, nose, and throat cancer: Ultrasound diagnosis of metastasis to cervical lymph nodes. Radiology 1984;152:771–773.

Chae SY, Jung HN, Ryoo I, Suh S. Differentiating cervical metastatic lymphadenopathy and lymphoma by shear wave elastography. Sci Rep 2019;9:12396.

Cheng KL, Choi YJ, Shim WH, Lee JH, Baek JH. Virtual Touch tissue imaging quantification shear wave elastography: Prospective assessment of cervical lymph nodes. Ultrasound Med Biol 2016;42:378–386.

Cooper JS, Porter K, Mallin K, Hoffman HT, Weber RS, Ang KK, Gay EG, Langer CJ. National Cancer Database report on cancer of the head and neck: 10-year update. Head Neck 2009;31:748–758.
Desmots F, Fakhry N, Mancini J, Reyre A, Vidal V, Jacquier A, Santini L, Moulin G, Varoquaux A. Shear wave elastography in head and neck lymph node assessment: Image quality and diagnostic impact compared with B-mode and doppler ultrasonography. Ultrasound Med Biol 2016;42:387–398.
Dragoni F, Cartoni C, Pescarmona E, Chiarotti F, Puopolo M, Orsi E, Pignoloni P, De Gregoris C, Mandelli F. The role of high resolution pulsed and color Doppler ultrasound in the differential diagnosis of benign and malignant lymphadenopathy: Results of multivariate analysis. Cancer 1999;85:2485–2490.
Ferlito A, Rinaldo A, Devaney KO, MacLennan K, Myers JN, Petruzzelli GJ, Shaha AR, Genden EM, Johnson JT, de Carvalho MB, Myers EN. Prognostic significance of microscopic and macroscopic extracapsular spread from metastatic tumor in the cervical lymph nodes. Oral Oncol 2002;38:747–751.
Fujiwara T, Tomokuni J, Iwanaga K, Ooba S, Haji T. Acoustic radiation force impulse imaging for reactive and malignant/metastatic cervical lymph nodes. Ultrasound Med Biol 2013;39:1178–1183.
Guruf A, Ozturk M, Bayrak IK, Polat AV. Shear wave versus strain elastography in the differentiation of benign and malignant breast lesions. Turk J Med Sci 2019;49:1509–1517.
He YP, Xu HX, Li XL, Li DD, Bo XW, Zhao CK, Liu BJ, Wang D, Xu HX. Comparison of Virtual Touch Tissue Imaging & Quantification (VTIQ) and Toshiba shear wave elastography (T-SWE) in diagnosis of thyroid nodules: Initial experience. Clin Hemorheol Microcirc 2017;66:15–26.
Heine D, Zenk J, Psychogios G. Two case reports of synchronous unilateral pleomorphic adenoma and cystadenolymphoma of the parotid gland with literature review. J Ultrasonogr 2018;18:369–373.
Herman J, Sedlackova Z, Furst T, Vachutka J, Salzman R, Vomacka J, Herman M. The role of ultrasound and shear-wave elastography in evaluation of cervical lymph nodes. BioMed Res Int 2019;2019 4318251.
Kau RJ, Alexiou C, Stimmer H, Arnold W. Diagnostic procedures for detection of lymph node metastases in cancer of the larynx. ORL Otorhinolaryngol Relat Spec 2000;62:199–203.
Kilic A, Colakoglu H, Er. Virtual touch tissue imaging quantification shear wave elastography for determining benign versus malignant cervical lymph nodes: A comparison with conventional ultrasound. Diagn Interv Radiol 2019;25:114–121.
Klintworth N, Mantsopoulos K, Zenk J, Psychogios G, Iro H, Bozzato A. Sonoelastography of parotid gland tumours: Initial experience and identification of characteristic patterns. Eur Radiol 2012;22:947–956.
Klotz T, Boussion V, Kwiatkowski F, Dieu-de Fraissinette V, Bailly-Glatre A, Lemery S, Boyer L. Shear wave elastography contribution in ultrasound diagnosis management of breast lesions. Diagn Interv Imaging 2014;95:813–824.
Lenghel LM, Bolboaca SD, Botar-Jid C, Baciut G, Dudea SM. The value of a new score for sonoelastographic differentiation between benign and malignant cervical lymph nodes. Med Ultrasonogr 2012;14:271–277.
Luo S, Kim EH, Dighe M, Kim Y. Thyroid nodule classification using ultrasound elastography via linear discriminant analysis. Ultrasonics 2011;51:425–431.
Mansour N, Bas M, Stock KF, Strassen U, Hofauer B, Knopf A. Multimodal ultrasonographic pathway of parotid gland lesions. Ultraschall Med 2017;38:166–173.
Mansour N, Bobenstetter L, Mansour S, Graf S, Hofauer B, Knopf A. [Differentiation of ultrasonographic hypoechoic head and neck lesions]. Laryngorhinootologie 2019;98:701–707.
Mantsopoulos K, Klintworth N, Iro H, Bozzato A. Applicability of shear wave elastography of the major salivary glands: Values in healthy patients and effects of gender, smoking and pre-compression. Ultrasound Med Biol 2015;41:2310–2318.
Matsuzuka T, Suzuki M, Saijo S, Ikeda M, Matsui T, Nomoto Y, Nomoto M, Imaizumi M, Tada Y, Omori K. Stiffness of salivary gland and tumor measured by new ultrasonic techniques: Virtual Touch quantification and IQ. Auris Nasus Larynx 2015;42:128–133.
McQueen AS, Bhatia KS. Head and neck ultrasound: Technical advances, novel applications and the role of elastography. Clin Radiol 2018;73:81–93.
Okasha HH, Mansour M, Attia KA, Khattab HM, Sakr AY, Naguib M, Aref W, Al-Naggar AA, Ezzat R. Role of high resolution ultrasound/endosonography and elastography in predicting lymph node malignancy. Endoscopic Ultrasound 2014;3:58–62.
Psychogios G, Rueger H, Jering M, Tsoures E, Kunzel J, Zenk J. Ultrasound can help to indirectly predict contact of parotid tumors to the facial nerve, correct intraglandular localization, and appropriate surgical technique. Head Neck 2019;41:3211–3218.
Pu H, Zhao LX, Yao MH, Xu G, Liu H, Xu HX, Wu R. Conventional US combined with acoustic radiation force impulse (ARFI) elastography for prediction of triple-negative breast cancer and the risk of lymphatic metastasis. Clin Hemorheol Microcirc 2017;65:335–347.
Rosen J, Brown JD, De S, Sinanan M, Hannaford B. Biomechanical properties of abdominal organs in vivo and postmortem under compression loads. J Biomech Eng 2008;130 021020.
Rubaltelli L, Proto E, Salmaso R, Bortoletto P, Candiani F, Cagol P. Sonography of abnormal lymph nodes in vitro: Correlation of sonographic and histologic findings. AJR Am J Roentgenol 1990;155:1241–1244.
Rüger H, Psychogios G, Jering M, Thölken R, Zenk J. Gleichartigkeit von Lymphomen und Benignomen in der Sonografie mit Virtual Touch Imaging Quantification (VTIQ). Laryngorhinootologie 2019;98:213.
Smith AJ. Lymph node issues in solid tumour management. J Surg Oncol 2009;99:173.
Steinkamp HJ, Cornehl M, Hosten N, Pegios W, Vogl T, Felix R. Cervical lymphadenopathy: Ratio of long- to short-axis diameter as a predictor of malignancy. Br J Radiol 1995;68:266–270.
Suh CH, Choi YJ, Baek JH, Lee JH. The diagnostic performance of shear wave elastography for malignant cervical lymph nodes: A systematic review and meta-analysis. Eur Radiol 2017;27:222–230.
Tan R, Xiao Y, He Q. Ultrasound elastography: Its potential role in assessment of cervical lymphadenopathy. Acad Radiol 2010;17:849–855.
Tozaki M, Saito M, Benson J, Fan L, Isobe S. Shear wave velocity measurements for differential diagnosis of solid breast masses: A comparison between Virtual Touch quantification and Virtual Touch IQ. Ultrasound Med Biol 2013;39:2233–2245.
Turgut E, Celenk C, Tanrivermis Sayit A, Bekci T, Gunbey HP, Aslan K. Efficiency of B-mode ultrasound and strain elastography in differentiating between benign and malignant cervical lymph nodes. Ultrasound Q 2017;33:201–207.
Ying M, Ahuja A, Metreweli C. Diagnostic accuracy of sonographic criteria for evaluation of cervical lymphadenopathy. J Ultrasound Med 1998;17:437–445.
Zenk J, Bozzato A, Steinhart H, Greess H, Iro H. Metastatic and inflammatory cervical lymph nodes as analyzed by contrast-enhanced color-coded Doppler ultrasonography: Quantitative dynamic perfusion patterns and histopathologic correlation. Ann Otol Rhinol Laryngol 2005;114:43–47.
Zhang YF, Xu HX, He Y, Liu C, Guo LH, Liu LN, Xu JM. Virtual Touch tissue quantification of acoustic radiation force impulse: A new ultrasound elastic imaging in the diagnosis of thyroid nodules. PloS One 2012;7:e49094.
Zhang JP, Liu HY, Ning CP, Chong J, Sun YM. Quantitative analysis of enlarged cervical lymph nodes with ultrasound elastography. Asian Pac J Cancer Prev 2015;16:7291–7294.
Zhang P, Zhang L, Zheng S, Yu C, Xie M, Lv Q. Acoustic radiation force impulse imaging for the differentiation of benign and malignant lymph nodes: A systematic review and meta-analysis. PloS One 2016;11 e0166716.
Zhao Y, Xi J, Zhao B, Xiong W, Jiang D, Yang L, Cai Z, Liu T, Jiang H, Rong S, Jin X. Preliminary evaluation of Virtual Touch tissue imaging quantification for differential diagnosis of metastatic and nonmetastatic cervical lymph nodes. J Ultrasound 2017;36:557–563.